# Visualization of Dendrimer Molecules by Transmission Electron Microscopy (TEM): Staining Methods and Cryo-TEM of Vitrified Solutions

**Catheryn L. Jackson,* Henri D. Chanzy,† Frank P. Booy,‡ Bartholomew J. Drake, Donald A. Tomalia,¶ Barry J. Bauer, and Eric J. Amis**

*Polymers Division, National Institute of Standards and Technology, Gaithersburg, Maryland 20899*

*Received April 20, 1998; Revised Manuscript Received June 23, 1998*

ABSTRACT: Individual dendrimer molecules of poly(amidoamine) (PAMAM) from generation 10 (G10) to G5 were imaged by conventional transmission electron microscopy (TEM) after staining with aqueous sodium phosphotungstate. The dendrimers were resolved as separate, beam-stable entities, and their sizes and distribution of sizes were statistically analyzed and compared with data from small-angle X-ray scattering in solution. Aqueous G10 dendrimers were also characterized by examination in the frozen, hydrated state after quench-freezing in liquid ethane (cryo-TEM) and the data compared with the results of the staining experiments. To a first approximation, the dendrimers appeared circular in projection and the diameters conformed to a Gaussian distribution which broadened somewhat with increasing generation number. Cryo-TEM, in general, confirmed the staining experiments but suggested that, in the native state, there is more variability in the shapes of the dendrimers, with polyhedral shapes occurring quite frequently.

## Introduction

The study of macromolecular or polymer morphology has followed divergent paths for synthetic[1] and biological[2] polymers, partly because of limited interaction between the synthetic and biological polymer communities and partly because of the very different chemical structure and solubility of each class of material. For example, synthetic polymers are often highly polydisperse, nonpolar, and soluble in organic solvents, while biological polymers are often monodisperse, polar (or highly functionalized), and soluble in water or very polar solvents. Dendrimers are one type of synthetic polymer that may bridge the gap quite naturally between the synthetic and biological polymer fields because they are nearly monodisperse, highly functionalized, and most often water soluble. In addition, some applications being investigated for dendrimers and hyperbranched polymers are directly related to biological areas of study; for example, the transfer of genetic material in cells[3,4] or the use of highly boronated, dendritic peptide markers for electron spectroscopic imaging of antigens.[5] Dendrimers and hyperbranched polymers have been extensively reviewed[6−8] with the emphasis primarily on the design and synthesis of these materials. In general, reports on new syntheses have greatly outpaced the characterization of physical properties or the identification of applications for dendritic molecules.

The literature contains very few images of dendrimers,[6,9,10] probably because their size range (2−15 nm) and fragile organic composition make the resolution of such objects by electron beam techniques very difficult. For example, images of eighth-generation poly(amidoamine) (PAMAM)[9] dendrimers (G8), designated as G*X* where *X* is the generation number, stained with osmium tetroxide have been obtained at low resolution by microtoming dried films of the dendrimers at low temperatures.[6] Cryomicrotomy produces a nominal thickness of 60 nm or greater, resulting in superposition of the layered dendrimers through the thickness of the film. Alternatively, PAMAM dendrimers of G9 were surface-modified and then stained with ruthenium tetroxide, but the images showed excessive clumping because of the method of preparation.[6] In general, the visualization of isolated polymer molecules of the synthetic variety is rare; most often they are observed in crystalline arrays or assemblies of many molecules using high-resolution electron microscopy[11,12] or atomic force microscopy.[13] In the case of dendrimers, the local density should be sufficient to create contrast with staining or in cryo-TEM (transmission electron microscopy) because the branched-chain architecture is compact. The possible compaction of linear chains was reported by Richardson[14] in the 1960s. In this case, the direct observation of linear polymer molecules sprayed from solution and shadowed with platinum was reported as a possible method of the determination of molecular weight. The technique was most useful for amorphous glassy polymers of very high (>1 million) molecular weight and thus is somewhat limited in utility.

Producing better images of dendrimer molecules may supply answers to fundamental questions such as whether dendrimers have truly uniform sizes, spherical shapes, and dense (or hollow) cores. The visualization of dendrimer assemblies would also be helpful to confirm the structure and morphology for many applications of dendrimers, such as self-assembled monolayers, incorporation of metal ions in dendrimer cavities, and production of quantum dots for applications in the electronics industry.[15] An example of images showing aggregation of amphiphilic block copolymers of polystyrene dendrimer has been recently reported, where spherical micelles, micellar rods, or vesicular structures formed, depending on the generation number.[16]

† CERMAV, CNRS, BP53, 38041 Grenoble Cedex 9, France.
‡ NIH, Laboratory of Structural Biology, NIAMS, Bethesda, MD 20892.
¶ Michigan Molecular Institute, Midland, MI 48640.

S0024-9297(98)00615-9 CCC: $15.00 
Published on Web 08/19/1998

The techniques of negative and positive staining,[2,17] widely used for biological systems, use an electron-dense heavy-metal salt in solution to provide contrast in the transmission electron microscope and to minimize problems of sample beam damage. In negative staining, the specimen is surrounded by the stain or "cast" and thus appears light in color, while in positive staining the particle reacts directly with the stain and appears dark. Another technique developed for biological specimens is cryo-TEM, where an aqueous solution of virus particles or proteins is vitrified and imaged directly in the TEM using a cold stage and cryotransfer station.[2,18] This permits the near-native structure to be observed without dehydration or staining, with control of environmental variables such as buffer, pH, and ionic strength. For synthetic polymers, the technique has been used to study complex fluids[19] (such as colloids) and polymer micelles.[20]

This work describes the feasibility of biological staining techniques in conventional TEM and cryo-TEM to study individual PAMAM dendrimer molecules.[21] From the stained images, the dendrimers are spherical to a first approximation and we compare the average size and size distribution of dendrimers G10 to G5 from TEM to size measurements made by other techniques, such as small-angle X-ray scattering (SAXS).[22] A lower size limit of about 4 nm was found for the resolution of the simple methods described here, which may be improved through energy filtering of the image. The cryo-TEM method was successfully used on the G10 dendrimers in vitrified water, giving a better represention of the native size and shape of the dendrimer molecules in solution. In some cryo-TEM images, the dendrimers self-assemble into ordered aggregates of two-dimensional clusters, where the dendrimers do not appear to interpenetrate even though they are in close proximity. However, it is possible that the clusters may form during the preparation of the specimen for cryo-TEM, as reported previously for biological particles.[2] The cryo-TEM images also show that although G10 dendrimers are roughly spherical, they appear more polyhedral or irregular than those observed for the stained dendrimers by conventional TEM. In the discussion, the potential of the cryo-TEM method for future studies on dendrimers in solution will be outlined.

## Experimental Section

The PAMAM dendrimers were synthesized by Dendritech[23] from a tetrafunctional core of ethylenediamine by successive additions of methyl acrylate and ethylenediamine following methods previously described.[6] The theoretical relative molecular masses, $M_r$, range from 934 720 g/mol for the 10th generation, G10, down to 28 800 g/mol for the fifth generation, G5. The dendrimers were received in methanol at mass fraction of ~25% and stored in a freezer when not in use. The methanol solution was first diluted in distilled water to a concentration of about 0.2 mg/mL. Some solutions were further diluted to a concentration of ~0.02 mg/mL in 0.01 mol/L HCl to protonate the terminal primary amine groups on the molecules or 0.1 mol/L NaCl to screen electrostatic interactions between molecules. The diluted solutions were stored in a refrigerator and used within 4 weeks of preparation.

To prepare stained specimens for conventional TEM, the dendrimer solutions were deposited on 400-mesh Formvar-free carbon-coated copper grids (Ted Pella Type-A; nominal carbon thickness 2−3 nm) and inverted on a drop of an aqueous sodium phosphotungstate (NaPTA) solution, which is a solution of phosphotungstic acid with a mass fraction of 2%, that has been neutralized with sodium hydroxide (to pH = 7). For G7 and smaller size dendrimers, ~1-nm-thick ultrathin carbon substrates were prepared on mica, floated onto water, and deposited on Formvar-free lacy carbon copper grids.[2] Prior to use, each grid was treated for 2−5 s in a glow-discharge tube in a partial vacuum to impart hydrophilic character to the carbon substrate.[13] Other stains were also investigated, including uranyl acetate, uranyl tungstate, methylamine tungstate, and sodium silicotungstate, and some of these are reported in the results.

The conventional TEM images were obtained at 80 kV with a Philips 400T at a magnification of 36 000× or less under low-dose conditions. For the size measurements, the microscope was calibrated under the same conditions using a negatively stained bacteriophage T4 virus, with a reported tail-sheath spacing of 4.06 nm.[24] The images of the dendrimers and T4 were accurately enlarged and printed on Kodak Kodabromide F5 paper, then scanned into the computer, and analyzed with NIH Image.

For cryo-EM experiments in the TEM, commercially available lacy carbon membranes on 300-mesh copper grids were used after washing under reflux with chloroform to remove the Formvar and then refluxing in acetone prior to use. A 5-$\mu$L sample of the dilute dendrimer solution was applied to the grid, blotted to a thin film with filter paper, and immediately plunged into liquid ethane (−186 °C) in a Reichert KF-80 cryo-station. A Gatan model 626 cryo-transfer station and cryo-holder were used to transfer the grid containing the vitrified suspension into a Philips CM120 or Philips 400T TEM. The imaging was performed at 100 kV with low-dose procedures and magnifications of up to 36 000×. To minimize beam damage, magnifications of 22 000× and lower were found to be the most suitable.

## Results and Discussion

The results of conventional TEM of stained dendrimers can describe the average size, shape, and size distribution for generations G10 to G5. Since a unique feature and advantage of the TEM is the ability to visualize individual molecules, the characterization of the size distribution is an important result of this work. Although other techniques such as viscosity measurements and scattering methods can measure the average size of dendrimers, information about the breadth of the distribution is less direct. In applications where dendrimer molecules of different sizes are mixed, TEM would be the technique of choice for characterization. Other areas where the maximum resolution of TEM imaging might be useful include the study of blends of dendrimers with other polymers and in assemblies of dendrimers with other molecules, such as in the use of dendrimers to transfer genetic material in cells.[3,4] To our knowledge, this is the first time that biological methods of staining and cryo-EM techniques have been applied to individual dendrimer molecules.

**a. Conventional TEM.** The positively stained PAMAM dendrimers are shown in Figure 1a−f for G10 to G5, respectively. The stain used in this case was NaPTA, which resulted in mostly positively stained regions on the grid. The dendrimer molecules appear as dark objects on a light background of the amorphous carbon substrate and they are well-separated from each other, facilitating size measurements with image analysis software. For G6 and G5, a small amount of G10 was added as a focusing aid, and a few of these molecules are seen in parts e and f of Figure 1, respectively. This greatly improved the ability to achieve the best focus in images for the smaller dendrimers. The shapes of the stained molecules are spherical to a first approximation for G10 to G7, with

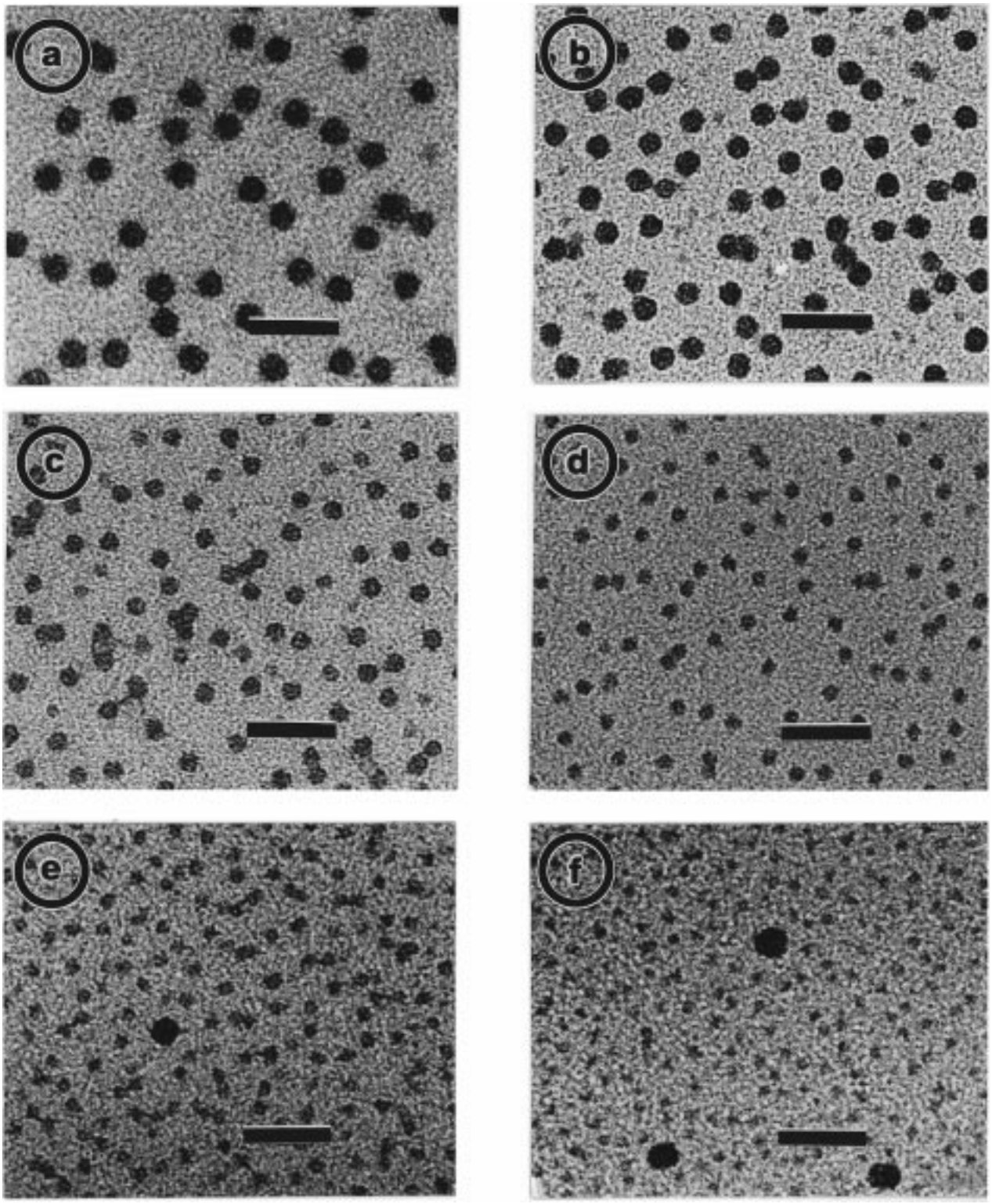


**Figure 1.** PAMAM dendrimers positively stained with 2% aqueous sodium phosphotungstate imaged by conventional TEM: (a) G10, (b) G9, (c) G8, (d) G7, (e) G6, (f) G5. The scale bars indicate 50 nm. For G6 and G5, a small amount of G10 has been added as a focusing aid; see text for details.

some molecules showing "edges" or slightly polyhedral shapes. For G6 and G5, the shapes become more indistinct because the grain of the carbon substrate is closer in size to the molecule and the edges become more difficult to delineate. The amount of stain taken up by the smaller dendrimers is probably also less, and these two factors limit the resolution of the technique.

Other stains could also be used to image the dendrimers as shown in Figure 2. G10 stained with methylamine tungstate, shown in Figure 2a, gave regions of both positive (white arrow) and negative (black arrow) type staining. In some regions of the negative stain, however, the molecules are clumped and overlapped, which makes size measurements difficult. An image of G9 in sodium silicotungstate is shown in Figure 2b. In this case, mostly positive staining occurs and the molecules look similar in size and shape to the result obtained with NaPTA. The G10 dendrimers

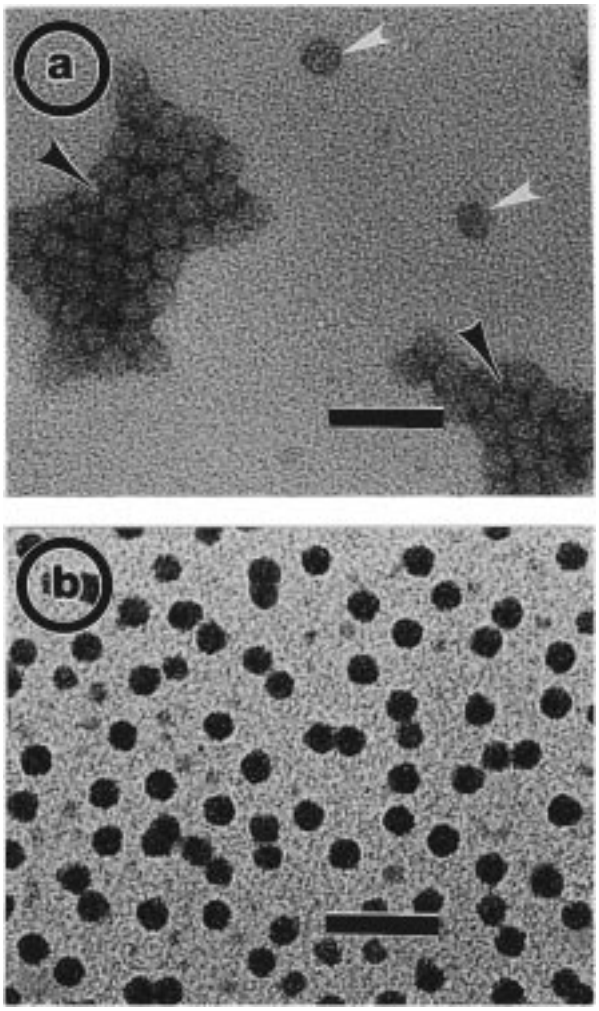


**Figure 2.** TEM images of PAMAM dendrimers: (a) G10 stained with 2% methylamine tungstate where both negatively stained regions (dark arrow) and positively stain regions (white arrow) are observed; (b) G9 stained with 2% sodium silicotungstate. The scale bars indicate 50 nm.

could also be imaged at 80 kV without stain; however, the contrast was much lower than that shown in Figures 1 and 2 for the stained G10 dendrimers.

Multiple images of the type shown in Figure 1 for dendrimers stained in NaPTA were used for the size measurements with the NIH Image software. Minimal image enhancement was done in the processing step using the smooth command or look-up table adjustments; however, thresholding of the image must be done before the size measurements can be obtained. The thresholding values were carefully adjusted to ensure that the background grain did not artificially enlarge the molecules (threshold too high) or erode the molecules (threshold too low). After an initial size measurement, the size range was set to eliminate the clumped and faded particles. The NIH Image program can measure the major and minor axes of an ellipse, and we found the average of these values to be a good estimate of the diameter calculated using an area measurement and assuming the dendrimers were spherical.

The mean and median diameters of each generation are listed in Table 1, along with the standard deviation of the measurement. In general, the agreement between the mean and median diameters is good, indicating that the distribution is approximately Gaussian in shape. The mean diameters range from 14.7 nm for G10 to 4.3 nm for G5. A histogram of the distribution of diameters is shown in Figure 3. Although it might be expected that the distribution would be skewed with a tail of smaller molecules, on the basis of the method of chemical synthesis,[6] we did not observe this in our measurements. In general, the size distributions are fairly narrow, but we observe a broadening at the higher generation numbers and especially for G10. Since more imperfections can occur as the generations are built up in the successive synthesis steps, it is not surprising that the size distribution broadens. MALDI-TOF mass spectrometry experiments have shown that PAMAM dendrimers beyond G7 have less than the theoretical molecular weight but still a narrow molecular weight distribution. Variations in size could also be due to different instantaneous configurations of the dendrimers in solution, even for monodisperse dendrimers.

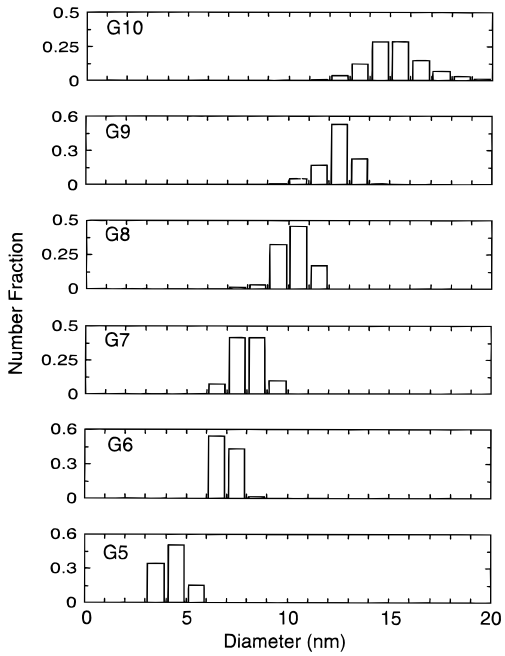


**Figure 3.** Histogram of the size distribution of diameters for PAMAM dendrimers from G10 down to G5: number fraction versus diameter in nanometers.

**Table 1. Size Measurements on PAMAM Dendrimers from Computer Analysis of TEM Images**

| generation | mean diameter (nm) | median diameter (nm) | no. of dendrimers | standard deviation |
|---|---|---|---|---|
| 10 | 14.7 | 14.8 | 413 | 1.1 |
| 9 | 12.4 | 12.5 | 1331 | 0.8 |
| 8 | 10.2 | 10.3 | 459 | 0.8 |
| 7 | 8.0 | 8.0 | 576 | 0.7 |
| 6 | 6.9 | 6.9 | 239 | 0.5 |
| 5 | 4.3 | 4.3 | 285 | 0.7 |

The mean diameters of the dendrimers measured by TEM on the stained specimens compare well with SAXS measurements in methanol by Prosa et al.,[22] as shown in Figure 4. The radius of gyration, $R_g$, measured by SAXS was converted to a sphere radius, $R$, assuming a uniform density sphere model, as $R = R_g/\sqrt{0.6}$. The close agreement between the techniques suggests that the staining done on wet dendrimer molecules locks in the size of the dendrimer in solution, which is the intent of staining a specimen in solution, since a dendrimer shrunken to bulk density would be smaller. More recent synchrotron SAXS measurements of G10 dendrimers also show a fairly narrow size distribution.[25]

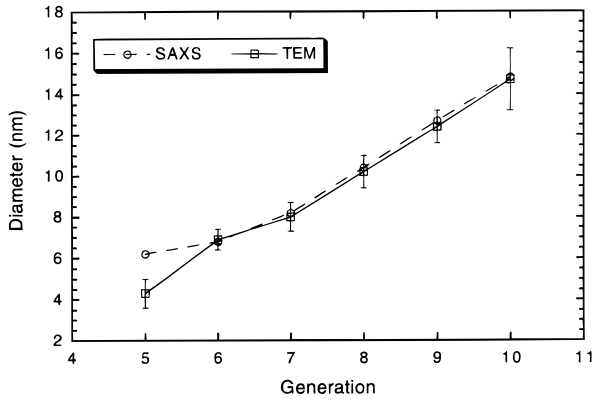


**Figure 4.** Comparison of mean dendrimer diameters measured by TEM (□) and small-angle X-ray scattering (○) techniques, as a function of generation number and molecular weight. The error bars for the TEM data represent 1 standard deviation (68% confidence interval for a normal distribution).

**b. Cryo-TEM.** The application of cryo-TEM to PAMAM dendrimers was successful for the largest dendrimer studied, G10, and the conventional TEM of the stained specimens and cryo-TEM results will be compared and contrasted, with a discussion of the limitations of both techniques. Such comparisons are common in the study of aqueous suspensions of particles by TEM, and reasonable agreement is generally found,[2,26,27] with a gain of complementary information. The comparison of these two techniques is sensible because cryo-TEM is a relatively new technique while negative staining has been in use for about 40 years.[2] In addition, because of inherently low image contrast in the cryo-TEM images and the variation in signal-to-noise depending on the thickness of the vitrified water layer, the degree of underfocus, and the beam sensitivity of unstained cryo specimens, a comparison with staining methods allows for adjustments in concentration and other variables to more quickly optimize the conditions for cryo-TEM. Some of the critical factors for interpreting cryo-TEM results include the sample concentration, the thickness of the vitrified layer, the mechanism of contrast and defocus, the effect of shear during the blotting step, surface effects of preparing a thin liquid layer, and beam damage.

The images of the G10 dendrimers in vitrified water are shown in Figure 5. In these and subsequent cryo-TEM images, no stain is used and the contrast is produced by the difference in density between the dendrimers and water, enhanced by phase-contrast effects resulting from under focusing of the objective lens (by about 1 $\mu$m).[15] The dendrimers are of a size in the cryo-TEM images similar to that observed in negative stain (Figure 2a), indicating that they do not change significantly when stained, but the shapes in the cryo-TEM images are more irregular. The G10 dendrimers in water often self-assemble into close-packed aggregates of two-dimensional clusters, where the dendrimers do not appear to interpenetrate even though they are in close proximity. In Figure 5a, the aggregate is about 17 dendrimers wide and the region of vitrified water occupied by the aggregate appears somewhat lighter in contrast than the surrounding region. This means that the vitrified film is thinner here than in the darker surrounding region and possibly that surface effects inherent to producing a very thin film may have induced the aggregate to form on the grid during the blotting and quenching steps. Thus, although the aggregate itself is not an artifact, it may not accurately represent the spatial arrangement of the dendrimers in solution prior to creating the vitrified water layer that spans the lacy carbon membrane. Because the dendrimer solution shown in Figure 5a appears to have a fairly high concentration of dendrimers, we initially thought that aggregate formation was, in part, due to the high concentration. Upon dilution, however, aggregates were still observed in regions of vitrified water which contained a much lower concentration of dendrimers, as seen in Figure 5b. In this case, the aggregates are 3−8 dendrimers wide and the thickness of the vitrified layer is more uniform throughout the entire region.

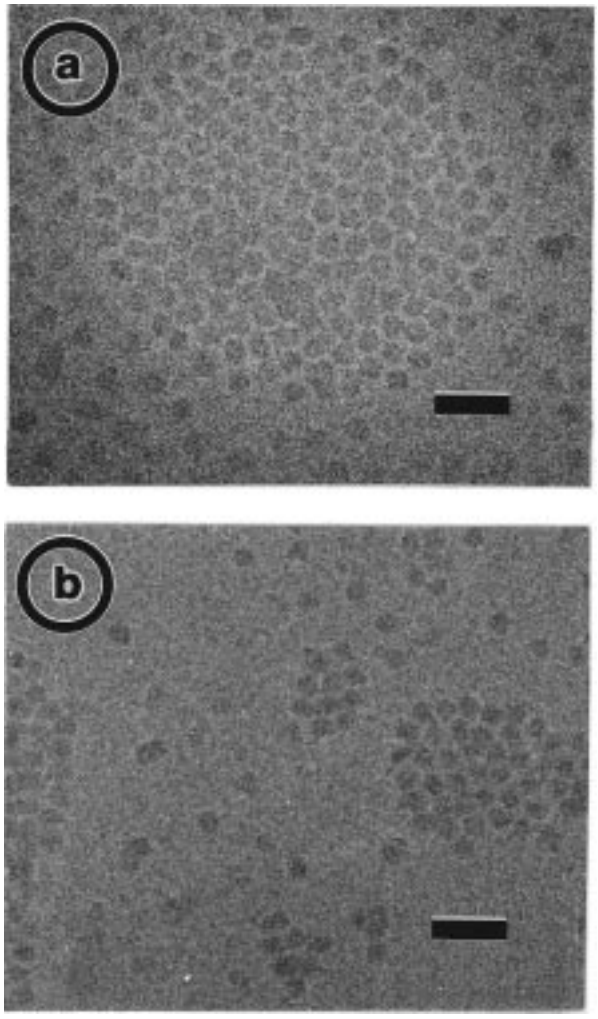


**Figure 5.** G10 dendrimers imaged in vitrified water by cryo-TEM showing clusters and lack of interpenetration of dendrimers: (a) large cluster of about 17 dendrimers wide in a higher concentration region; (b) smaller clusters of about 3−8 dendrimers wide in a lower concentration region. The scale bars indicate 50 nm.

The projected shapes of the G10 dendrimers in Figure 5 do not appear strictly circular, especially when examined within the large aggregate in Figure 5a, where the vitrified layer is thinner and the contrast between the molecules and matrix is somewhat higher. Because the formation of the aggregate in the vitrified layer may deform the dendrimer shapes, we tried to observe the dendrimers in a more dilute region and, where possible, with higher contrast between the individual dendrimers and the vitrified water. We found that by adding acid to the water solution to protonate

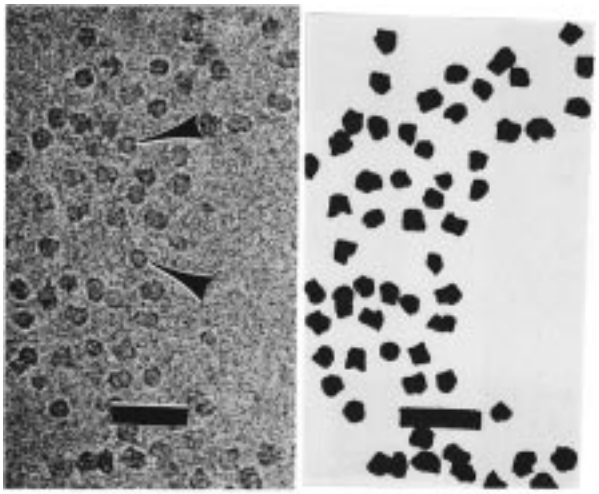


**Figure 6.** (a) G10 dendrimers in dilute HCl imaged by cryo-TEM in vitrified solution. (b) Schematic tracing of dendrimer shapes from the image. Arrows indicate molecules that appear hollow because of artifact of the defocusing conditions; see text for discussion. The scale bar indicates 50 nm.

the primary amine groups on the terminal units of the molecules, the dendrimers tended to clump less, as shown in Figure 6. Also, by imaging at a lower magnification of 22 000×, images were obtained of dendrimers in the vitrified solution which had more distinct boundaries than those observed in Figure 5. In Figure 6, the dendrimers are well-separated but still have polyhedral shapes, as shown in the side inset, and the shapes are not affected by the amount of defocus. This result implies that the shapes seen in the aggregates in Figure 5 are not produced during the formation of the aggregates, or because the dendrimers are in close proximity, but are the inherent shapes of the molecules in the vitrified solution. We also note that some of the molecules may appear hollow, as indicated by the arrows, but this is probably an artifact of the defocusing conditions, which produces a ring around the edge of the objects. Since the dendrimers are synthesized from a core of ethylenediamine, it is reasonable to suppose that some might retain the tetrahedral shape of the core molecule. In the future, simple tilting experiments or more complex 3D reconstruction methods might be useful to better analyze the shapes, but the quality of the current images did not warrant this analysis.

Working at lower magnification has both advantages and disadvantages; for example, it is more difficult to see the molecules and focus correctly at 22 000×. The images seen in Figure 5 taken at higher magnification are somewhat faded, however, as a result of radiation damage. This effect has been well-documented in the case of capsids of herpes simplex virus,[28,29] where multiple exposures of the same region show that the sharp edges of the particles become blurred at higher cumulative doses. Because the PAMAM dendrimers are amorphous molecules made by synthetic chemical routes, the structural information gathered here is primarily limited to the size and shape of the molecules in vitrified suspension. For biological particles, particularly those with high symmetry such as icosahedral viruses, a full 3D reconstruction may be calculated, since each view represents a symmmetry-related projection of an identical object.[28,29] Because the dendrimer molecules are

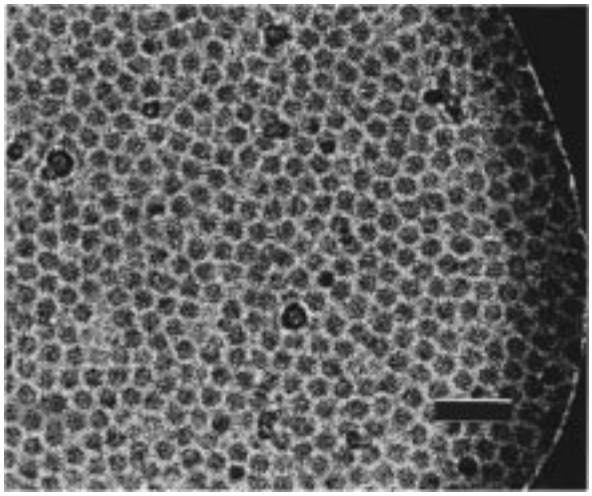

**Figure 7.** G10 dendrimers imaged in dilute NaCl by cryo-TEM in vitrified solution. The dark outline at the right is a contour of the lacy carbon membrane used as a support for the vitrified liquid layer. The scale bar indicates 50 nm.

variable in size, it is unlikely that they are identical and thus such a reconstruction cannot be calculated.

Cryo-TEM of the dendrimers in a dilute salt solution shows an example of a close-packed structure, as seen in Figure 7, where the dendrimers again have polyhedral shapes. Initially, we thought that the close-packed structure was the result of a high solution concentration. However, we found that upon dilution the salt solutions behaved differently than the water or dilute HCl solutions, in that distinct regions of high concentration, such as those shown in Figure 7, could coexist with regions containing no dendrimers at all in the vitrified layer. The salt is supposed to screen charges between the molecules, but because the blotting step is somewhat uncontrolled, there is no guarantee that the solution concentration of either salt or dendrimer is unchanged after blotting. The specimen may be partially dry or not fully embedded in the frozen buffer, as evidenced by the much greater contrast in Figure 7 compared to Figure 5 or Figure 6. This is usually a result of over blotting or solvent evaporation prior to freezing.

## Conclusions

Conventional TEM has been used to characterize the size, shape, and size distribution of individual molecules of PAMAM dendrimers from G10 to G5, using biological staining techniques. From the stained images, the dendrimers are spherical to a first approximation and the average sizes measured by TEM are consistent with SAXS results from dilute solutions. A lower size limit of about 4 nm was found for the easy visual recognition of the dendrimers in this study. To advance beyond this resolution, ever more care would be required to record closer-to-focus images at a lower electron dose. This would reduce image contrast and probably necessitate more sophisticated image analysis, although it is possible that the use of an energy filter to remove inelastically scattered electrons would help directly. In general, the size distributions are fairly narrow, but we observe a broadening at the higher generation numbers and especially for G10.

Cryo-TEM methods were successfully used to visualize the G10 molecules in vitrified water, which should more closely imitate the behavior in solution. The cryo-TEM images show that the G10 molecules are roughly

spherical but appear more polyhedral or irregular than those observed for the dendrimers in stain. In addition, the dendrimers sometimes self-assemble into ordered aggregates, where the molecules do not appear to interpenetrate even though they are in close proximity. The aggregates may not be typical of the structure in solution, however, as aggregation may occur during the preparation of the specimen for cryo-TEM. The cryo-TEM method has the potential to study interactions of these molecules as a function of ionic charge, salt content, and pH, but artifacts produced by shear in the blotting step, surface tension in the thin liquid layer, size segregation, and variation in the concentration may limit the usefulness of the method.[19] Use of a controlled environment vitrification system (CEVS),[19] to control relative humidity and water loss during preparation as well as to allow for reequilibration after the blotting step, may be useful to eliminate some of these artifacts and to allow the study of interactions.

**Acknowledgment.** We thank Dr. A. Steven at NIH for use of the cryo-microscopy laboratory and for making this collaboration possible. NIST collaborators on dendrimer related projects are acknowledged for their input during the course of this work, including Drs. J. F. Douglas, C. C. Han, A. Karim, A. I. Nakatani, T. J. Prosa, and A. Topp. H.D.C. acknowledges NIST for financial support as a guest scientist for 9 months in 1996−97. This work was supported in part by the U.S. Army Research Office under Grant 35109-CH.

## References and Notes

(1) Sawyer, L. C.; Grubb, D. T. *Polymer Microscopy*; Chapman and Hall: London, 1987.
(2) Harris, J. R. *Negative Staining and Cryoelectron Microscopy: the thin film techniques*; Bios Scientific Publishers: Oxford, U.K., 1997.
(3) Kukowskalatallo, J. F.; Bielinska, A. U.; Johnson, J.; Spindler, R.; Tomalia, D. A.; Baker, J. R. *Proc. Natl. Acad. Sci. U.S.A.* **1996**, *93*, 4897.
(4) Plank, C.; Mechtler, K.; Szoka, F. C.; Wagner, E. *Hum. Gene Ther.* **1996**, *7*, 1437.
(5) Qualman, B.; Kessels, M. M.; Klobasa, F.; Jungblut, P. W.; Sierralta, W. D. *J. Microsc.* **1996**, *183*, 69.
(6) Tomalia, D. A.; Naylor, A. M.; Goddard, W. A. *Angew. Chem., Int. Ed. Engl.* **1990**, *29*, 138.
(7) Frechet, J. M. J.; Hawker, C. J.; Gitsov, I.; Leon, J. W. *J. Macromol. Sci., Pure Appl. Chem.* **1996**, *A33*, 1399.
(8) Ardoin, N.; Astruc, D. *Bull. Soc. Chim. Fr.* **1995**, *132*, 875.
(9) Tomalia, D. A.; Baker, H.; Dewald, J.; Hall, M.; Kallos, G.; Martin, S.; Roeck, J.; Ryder, J.; Smith, P. *Macromolecules* **1986**, *19*, 2466.
(10) Newkome, G.; Moorefield, C. N.; Baker, G. R.; Saunders, M. J.; Grossman, S. H. *Angew. Chem., Int. Ed. Engl.* **1991**, *30*, 1178.
(11) Tsuji, M.; Kohjiya, S. *Prog. Polym. Sci.* **1995**, *20*, 259.
(12) Wu, J.; Lieser, G.; Wegner, G. *Adv. Mater.* **1996**, *8* (2), 151.
(13) Stocker, W.; Schumacher, M.; Graff, S.; Thierry, A.; Wittmann, J.-C.; Lotz, B. *Macromolecules* **1998**, *31*, 807.
(14) Richardson, M. J. *Proc. R. Soc. London, A* **1964**, *279*, 50.
(15) Balogh, L.; Swanson, D. R.; Spindler, R.; Tomalia, D. A. *Polym. Mater. Sci. Eng.* **1997**, *77*, 118.
(16) van Hest, J. C. M.; Delnoye, D. A. P.; Baars, M. W. P. L.; van Genderen, M. H. P.; Meijer, E. W. *Science* **1995**, *268*, 1592.
(17) Harris, J. R.; Horne, R. W. *Micron*, **1994**, *25*, 5.
(18) Dubochet, J.; Adrian, M.; Chang, J. J.; Homo, J. C.; Lepault, J.; McDowall, A. W.; Schultz, P. *Quart. Rev. Biophys.* **1988**, *21*, 129.
(19) Talmon, Y. *Ber. Bunsen-Ges. Phys. Chem.* **1996**, *100*, 364.
(20) Oostergetel, G. T.; Esselink, F. J.; Hadziioannou, G. *Langmuir* **1995**, *11*, 3721.
(21) Jackson, C. L.; Chanzy, H. D.; Booy, F. P.; Tomalia, D. A.; Amis, E. J. *Polym. Mater. Sci. Eng.* **1997**, *77*, 222.
(22) Prosa, T. J.; Bauer, B. J.; Amis, E. J.; Tomalia, D. A.; Scherrenberg, R. *J. Polym. Sci., Part B: Polym. Phys.* **1997**, *35*, 2913.
(23) All commercial equipment, instruments, and materials are identified in this paper in order to adequately specify the experimental procedure. However, such identification does not imply recommendation or endorsement by the National Institute of Standards and Technology, nor does it imply that materials and equipment identified are necessarily the best available for the purpose.
(24) Moody, M. F.; Malkowski, L. *J. Mol. Biol.* **1981**, *150*, 217.
(25) Prosa, T. J.; et al., in preparation.
(26) Booy, F. P. Cryoelectron Microscopy. In *Viral Fusion Mechanisms*; Bentz, J., Ed.; CRC Press: Boca Raton, FL, 1993; Chapter 2.
(27) Stewart, M.; Vigers, G. *Nature* **1996**, *319*, 631.
(28) Special issue on "Advances in Computational Image Processing for Microscopy": Carragher, B., Smith, P. R., Guest Eds. *J. Struct. Biol.* **1996**, *16*, 1−249.
(29) *Three-dimensional Electron Microscopy of Macromolecular Assemblies*; Frank, J., Ed.; Academic Press: New York, 1996.

MA9806155